Final Report: Grant No. DE-FG02-10ER16165 "Design of Stratified Functional Nanoporous Materials for CO_2 Capture and Conversion"

J. Karl Johnson, University of Pittsburgh, 27 September 2017

The objective of this project is to develop novel nanoporous materials for CO_2 capture and conversion. The motivation of this work is that capture of CO_2 from flue gas or the atmosphere coupled with catalytic hydrogenation of CO_2 into valuable chemicals and fuels can reduce the net amount of CO_2 in the atmosphere while providing liquid transportation fuels and other commodity chemicals.[1-6] One approach to increasing the economic viability of carbon capture and conversion is to design a single material that can be used for both the capture and catalytic conversion of CO_2, because such a material could increase efficiency through process intensification. We have used density functional theory (DFT) methods to design catalytic moieties that can be incorporated into various metal organic framework (MOF) materials. We chose to work with MOFs because they are highly tailorable, can be functionalized, and have been shown to selectively adsorb CO_2 over N_2, which is a requirement for CO_2 capture from flue gas. Moreover, the incorporation of molecular catalytic moieties into MOF, through covalent bonding, produces a heterogeneous catalytic material having activities and selectivities close to those of homogeneous catalysts, but without the draw-backs associated with homogeneous catalysis.

We have primarily investigated the use of Lewis pair functional moieties as catalytic groups for incorporation into various MOFs. Lewis pairs (LPs) contain both a Lewis acid and base site on the same molecular fragment. We have designed and screened many LPs for their potential to heterolytically dissociate H_2 into hydridic (bound to the Lewis acid) and a protic (bound to the Lewis base) species.[7,8] We then computed energetics and barriers for hydrogenation of CO_2 through a concerted 2-H addition to make formic acid. We have also computed reaction pathways for CO_2 to methanol through a series of 2-H addition steps.[9] We have found that the concerted addition of 2-H to CO_2 generally has barriers that are lower than for typical heterogeneous metal catalysts.[10-13]

We initially focused on the UiO-66 MOF because it is chemically and thermally stable,[14-19] selective toward CO_2 adsorption over N_2,[16,20-23] and can be readily functionalized via various approaches.[14,15,17,20-22,24-28] We proposed a LP moiety attached to the 1,4-benzenedicarboxylate (BDC) linkers of the UiO-66 framework and provided a plausible synthetic pathway for synthesis of this material.[29] The functionalized UiO-66 and linker are shown in Fig. 1. We initially constructed a family of functional groups by changing the R group on the LP moiety in Fig. 1(b). Eight different structures were generated using R = H, F, Cl, Br, CN, CH_3, CF_3, and NO_2. These groups were chosen to span a range of electron withdrawing potentials and steric effects. Reaction pathways for H_2 dissociation and CO_2 hydrogenation were computed for each of these materials. We constructed linear scaling relationships to model the transition states. We found that the transition states for H_2 dissociation scale linearly with the chemical

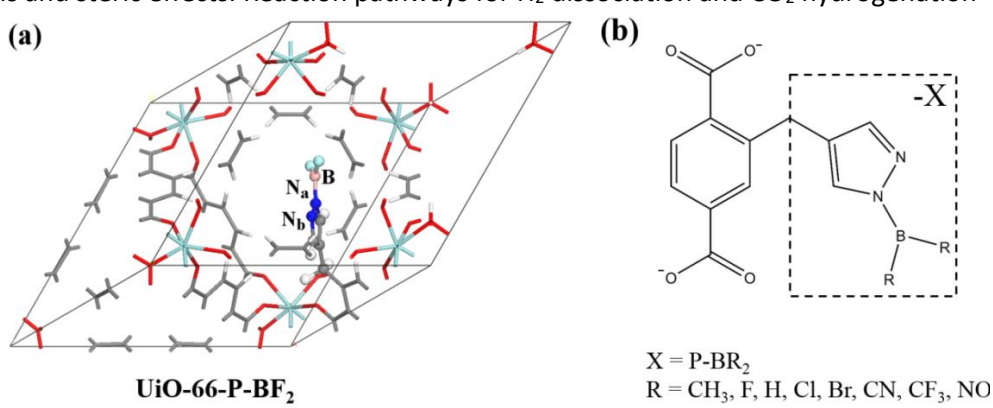

Fig. 1. Lewis Pair functionalized UiO-66 (UiO-66-X): (a) Primitive cell of UiO-66-P-BF_2, (b) BDC linker with Lewis pair functional group, where X represents the Lewis pair with different R substituents.

hardness of the Lewis acid site. The CO_2 hydrogenation barrier scales linearly with the H_2 chemisorption energy. We used these two scaling relations to construct a Sabatier plot in order to identify the optimum values of chemical hardness and H_2 adsorption energies for increasing the overall reaction rate. The Sabatier plot for this work is shown in Fig. 2.

The Sabatier plot in Fig. 2 was constructed using a limited number of functional groups all based on the P-BR_2 moiety shown in Fig. 1(b). One draw-back of this family of functional groups is that CO_2 generally binds to the LP groups with about the same or greater binding energy than H_2, meaning that CO_2 competes with H_2 for the catalytic sites, reducing the overall reaction rate. We therefore expanded our search for catalytically active LP functional groups by taking the approach of modeling just the gas phase LP clusters, computing H_2 and CO_2 binding energies and also reaction pathways for those groups having the most promising properties. We screened five different classes of functional groups, illustrated in Scheme 1, to test the hypothesis that changing the acidity or basicity of the LP moieties could be used to tune the relative binding energies of CO_2 and H_2.[8] Hence, this screening process was aimed at identifying functional groups that would selectively dissociate H_2 over binding CO_2, hence increasing the overall activity of the catalyst. We screened a total of 105 functional groups. We found that binding energies

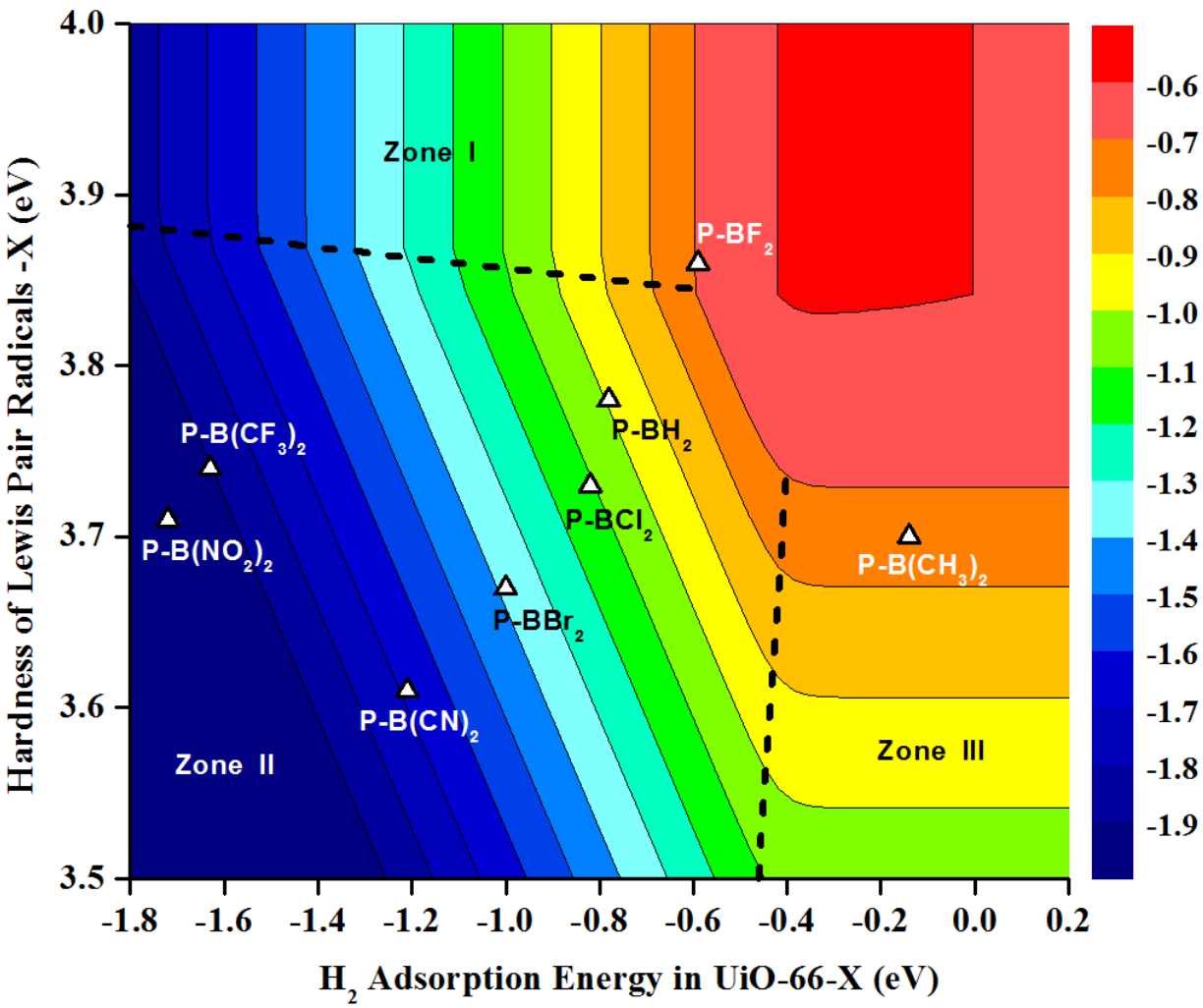

Fig. 2. Contour plot of the Sabatier activity for the overall reaction rate for CO_2 hydrogenation at 298 K. The CO_2 hydrogenation barrier is given by a BEP relationship with the H_2 adsorption energy and the H_2 dissociation barrier is given by a relationship with the hardness of the LP radicals -X. Specific LP groups are labeled on the figure. Figure taken from Ye and Johnson.[7]

indeed could be tuned by changing the acidity and the geometry of the LP functional groups. However, the functional groups having H_2 binding energies that were significantly larger than CO_2 binding energies were also seen to have unacceptably larger barriers for CO_2 hydrogenation, and hence none of the functional groups screened in this work were found to be promising.[8]

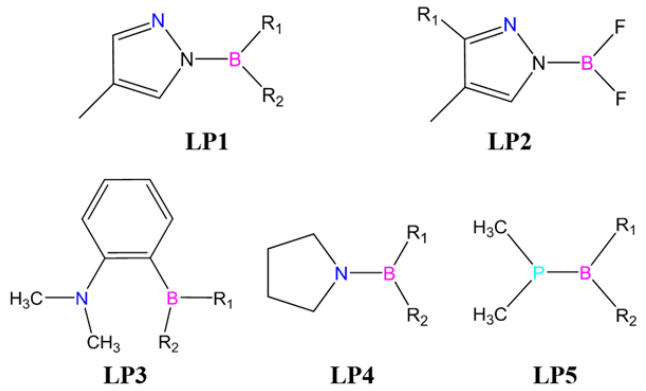

Scheme 1. **LP1**, **LP2**, **LP3**, **LP4** and **LP5** represent five families of Lewis pairs with different combinations of R_1 and R_2 substitutes. Lewis acid sites are B in pink, and Lewis base sites are N in blue or P in light blue. For **LP1**, R_1=R_2= H, F, Cl, Br, CN, CF_3, NO_2, NH_2, OH, OCH_3, CH_3 and phenyl, or R_1= F, Cl, Br, CN, CF_3 in combination with R_2= NH_2, OH, OCH_3, CH_3 and phenyl. For **LP2**, R_1= H, F, Cl, Br, CN, CF_3, NO_2, NH_2, OH, OCH_3, CH_3 and phenyl. For **LP3**, **LP4** and **LP5**, R_1=R_2= F, Cl, Br, CN, CF_3 and NO_2. Taken from Ye et al.[8]

We next turned to modifying the MOF and searching for confinement effects that could help tune the relative binding of CO_2 and H_2. We have investigated confinement and topology effects due to the architecture of the MOF by studying three different MOFs: UiO-67,[9] MIL-140B, and MIL-140C. The UiO-67 linker is 4,4' biphenyl-dicarboxylate (BPDC) linker, which is larger than the benzene dicarboxylate linker used in UiO-66. However, we utilized confinement in functionalized UiO-67 by incorporating the LP functional group into the linker, such that the Lewis base site is adjacent to the secondary building unit (SBU) ZrO cluster. This proximity to the SBU results in binding of CO_2 being sterically hindered.[9] The larger pore of UiO-67 also provides room for multiple LP functional groups per pore. We studied a functionalized MOF having four LP functional groups per pore, which we denote UiO-67-$(NBF_2)_4$. Multiple functional groups per pore provides the opportunity for multiple hydrogenation events without significant diffusion of the species being hydrogenated. Hence, we were able to compute reaction pathways for CO_2 hydrogenation to CH_3OH. We found multiple pathways for this overall reaction. The lowest barrier pathway proceeds via a series of simultaneous transfer of two hydrogens to produce methanol:

$$CO_2 \xrightarrow{+H_2} HCOOH \xrightarrow{+H_2} CH_2(OH)_2 \xrightarrow{-H_2O} CH_2O \xrightarrow{+H_2} CH_3OH.$$

This pathway involves four transition states (not counting the hydrogenation of the UiO-67-$(NBF_2)_4$). The self-condensation of $CH_2(OH)_2$ to CH_2O and H_2O in the lowest energy pathway can be catalyzed by a carboxylic acid functional group bound to the UiO-67 linker, which can be incorporated into the UiO-67-$(NBF_2)_4$ framework, producing a multi-functional catalyst. The potential energy surfaces for the various pathways are shown in Fig. 3. The transition states for this reaction are shown schematically in Fig. 3 as TS3, TS4, TS10, and TS11, having barrier heights of 0.53, 0.32, 0.6, and 0.32 eV, respectively. These barriers are all low enough to have significant rates at room temperature. Hence, the multifunctional UiO-67 catalyst should be active for CO_2 hydrogenation to methanol under mild conditions of temperature and pressure.

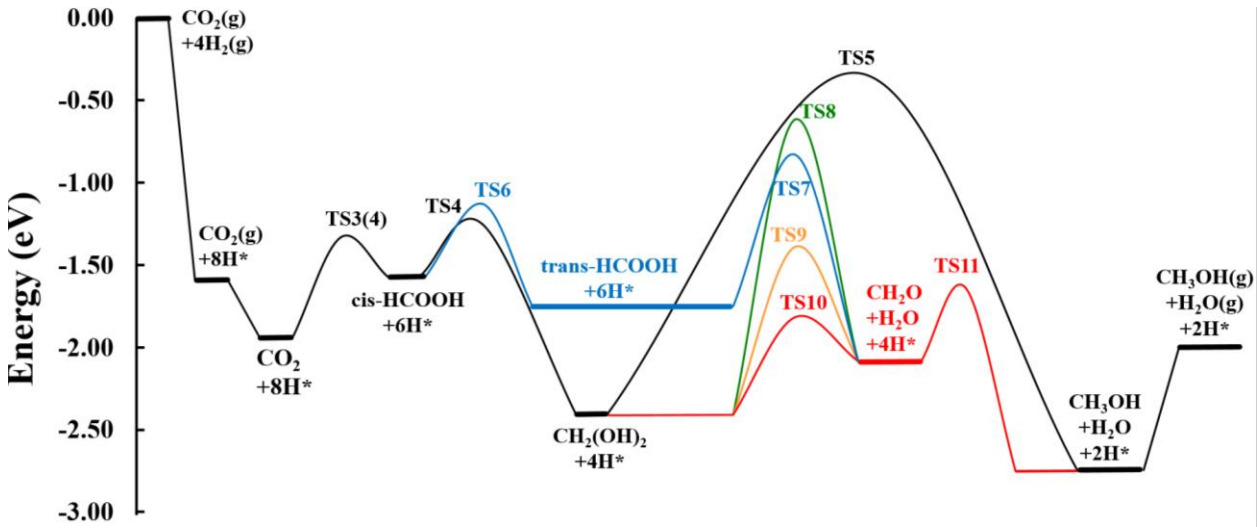

Fig. 3. Potential energy profiles for CO_2 hydrogenation to produce CH_3OH in UiO-67-$(NBF_2)_4$. Black: direct $CH_2(OH)_2$ hydrogenation to produce CH_3OH (all other pathways go through CH_2O as the intermediate to form CH_3OH); blue: cis-HCOOH→trans-HCOOH→CH_2O, green: self-decomposition of $CH_2(OH)_2$ to CH_2O; yellow: conversion of $CH_2(OH)_2$ to CH_2O catalyzed by H_2O; red: conversion of $CH_2(OH)_2$ to CH_2O catalyzed by a carboxylic acid functional group in the pore. Figure taken from Ye and Johnson.[9]

We also investigated MIL-140B and MIL-140C, which are MOFs having very different topologies than UiO-66 and Ui-67. The MIL family of materials have triangular shaped pores, with the MIL-140B material having the smallest pores. The structures of functionalized MIL-140B and MIL-140C are shown in Fig. 4. The smaller pores of MIL-140B are more highly confining, having greater steric hindrance, but it is the topology of the linker that has the biggest impact on the reaction pathways for CO_2 hydrogenation in these materials. The linker in MIL-140B is 2,6-naphthalenedicarboxylate (2,6-NDC) linker of MIL-140B, which has a fused ring topology (see Fig. 4b). This linker is less flexible than the BPDC linkers of MIL-140C. Because of this, the binding energies for CO_2 on MIL-140B and MIL-140C are -0.32 and 0.62 eV, respectively. We have shown that the increased binding energy for CO_2 on MIL-140C is due to the increased rotational flexibility of the BPDC linker.[30] The functionalized MIL-140B also has to reaction pathways for CO_2 hydrogenation, one of which involves a pre-activated CO_2 complex that is slightly bent. The overall reaction barrier for the pre-activated pathway is 0.15 eV lower than the pathway not involving the pre-activated bent CO_2. Conversely, although it is possible to find a pre-activated state for the MIL-140C material, the overall barrier is actually higher than going through the non-pre-activated pathway. Thus, there is a complex relationship between topology and confinement in the MOFs that cannot be predicted from cluster calculations for these materials.

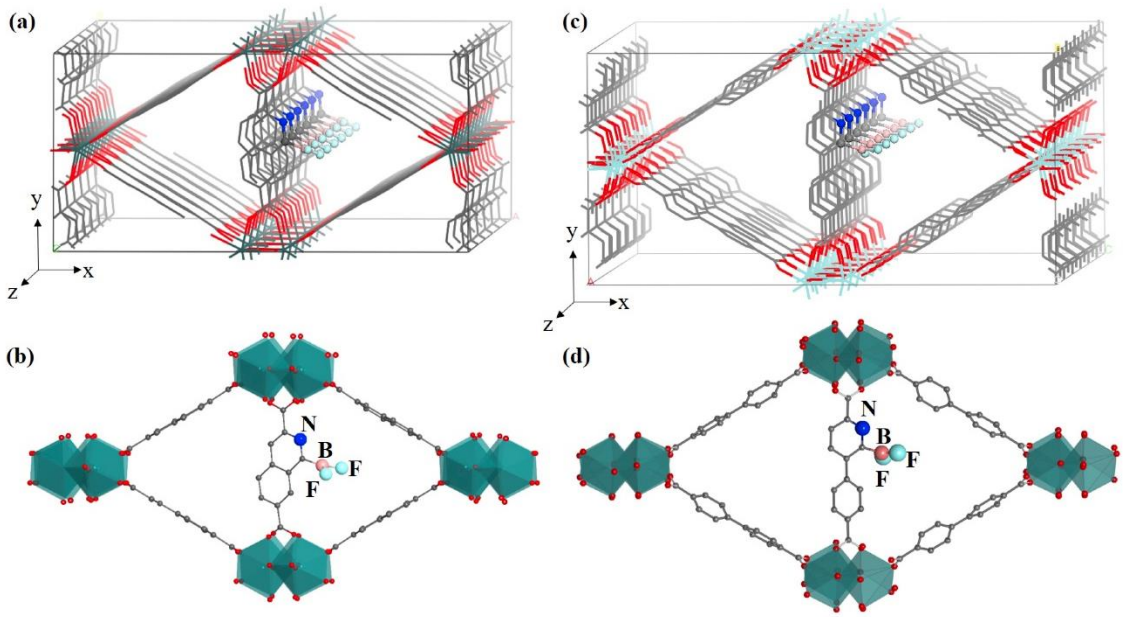

Fig. 4. Structures of MIL-140B-NBF_2 and with MIL-140C-NBF_2. Parts (a) and (c) illustrate the framework showing six unit cells along the *z* direction. The framework atoms are represented by lines, and the LP functional moieties are represented by balls and sticks. Colors of the atoms are as follows: pink for B, grey for C, blue for N, red for O, light cyan for F, dark green for Zr. Parts (b) and (d) show unit cells of MIL-140B-NBF_2 and with MIL-140C-NBF_2 with Zr represented by polyhedral and the other atoms represented by balls and sticks. Hydrogen atoms are not shown for clarity.

We are currently investigating a new class of catalytic MOF that have single atom metal hydrides as the active site. We generated a Cu-H chelated to a functionalized UiO-67 linker through a catecholate functional group, shown in the left-most panel of Fig. 5. This is a very different approach than the LP functionalized MOFs we have investigated in our previous work. Our preliminary results indicate that there is a low energy pathway for inserting CO_2 between the metal and hydride, leading to a formate species. The formate initially binds to the Cu site in a monodentate configuration, but can reconfigure to a lower energy bidentate structure through a low-barrier pathway. Subsequent addition of H_2 regenerates the metal hydride and adds a proton to the formate to produce formic acid. The rate limiting step is desorption of the formic acid, which is bound to the Cu atom. The desorption energy is about 0.85 eV. The potential energy diagram for this material is shown in Fig. 6.

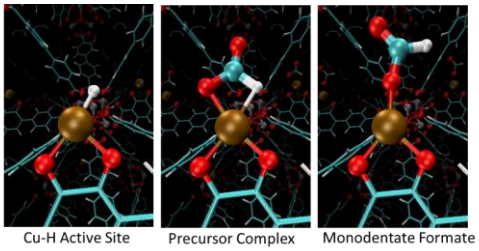

Fig. 5. Cu-hydride functionalized UiO-67 (left). Precursor complex of active site with CO_2 (middle). Inserted CO_2 monodentate formate complex (right).

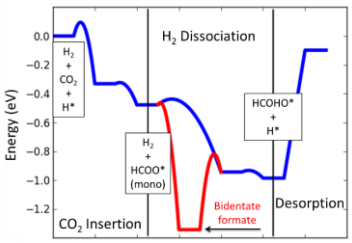

Fig. 6. Energy profile for CO_2 insertion and H_2 addition for the Cu-H catecholate functionalized UiO-67.

In summary, we have designed multiple materials that show promise for converting CO_2 to valuable products and which have the potential to be used to selectively capture CO_2 from flue gas.

Students and Postdocs Supported on this Grant

Postdoc: Jingyun Ye

Postdoc: Lin Li

Publications Resulting from the Grant

Jingyun Ye and J. Karl Johnson, "Design of Lewis Pair-Functionalized Metal Organic Frameworks for CO_2 Hydrogenation", *ACS Catalysis*, **5**, 2921-2928 (2015). DOI: 10.1021/acscatal.5b00396

Jingyun Ye, J. Karl Johnson "Screening Lewis Pair Moieties for Catalytic Hydrogenation of CO_2 in Functionalized UiO-66", *ACS Catalysis*, **5**, 6219-6229 (2015). DOI: 10.1021/acscatal.5b01191

Jingyun Ye, J. Karl Johnson, "Catalytic Hydrogenation of CO_2 to Methanol in a Lewis Pair Functionalized MOF", *Catalysis Science & Technology*, **6**, 8392-8405 (2016). DOI: 10.1039/c6cy01245k

Jingyun Ye, Benjamin Y. Yeh, Ronald A. Reynolds, J. Karl Johnson, "Screening the Activity of Lewis Pairs for Hydrogenation of CO_2", *Molecular Simulation*, **43**, 821-827 (2017).
DOI: 10.1080/08927022.2017.1295457

Jinyun Ye, Lin Li, J. Karl Johnson, "The Effect of Topology in Lewis Pair Functionalized Metal Organic Frameworks on CO_2 Adsorption and Hydrogenation", to be submitted to *The Journal of Physical Chemistry C* (2017).

Lin Li, J. Karl Johnson, "CO_2 Reduction on Metal Organic Framework with Metal Hydride Moieties", in preparation.

References

(1) Olah, G. A.; Prakash, G. S.; Goeppert, A. *J. Am. Chem. Soc.* **2011**, *133*, 12881.

(2) Dibenedetto, A.; Angelini, A.; Stufano, P. *J. Chem. Technol. Biotechnol.* **2014**, *89*, 334.

(3) Izumi, Y. *Coord. Chem. Rev.* **2013**, *257*, 171.

(4) Lim, R. J.; Xie, M.; Sk, M. A.; Lee, J.-M.; Fisher, A.; Wang, X.; Lim, K. H. *Catal. Today* **2014**, *233*, 169.

(5) Ma, J.; Sun, N.; Zhang, X.; Zhao, N.; Xiao, F.; Wei, W.; Sun, Y. *Catal. Today* **2009**, *148*, 221.

(6) Qiao, J.; Liu, Y.; Hong, F.; Zhang, J. *Chem. Soc. Rev.* **2014**, *43*, 631.

(7) Ye, J.; Johnson, J. K. *ACS Catal.* **2015**, *5*, 6219.

(8) Ye, J.; Yeh, B. Y.; Reynolds, R. A.; Johnson, J. K. *Mol. Simul.* **2017**, 1.

(9) Ye, J.; Johnson, J. K. *Catal. Sci. Technol.* **2016**, *6*, 8392.

(10) Ye, J.; Liu, C.-j.; Mei, D.; Ge, Q. *J. Catal.* **2014**, *317*, 44.

(11) Ye, J.; Liu, C.; Ge, Q. *J. Phys. Chem. C* **2012**, *116*, 7817.

(12) Peng, G.; Sibener, S. J.; Schatz, G. C.; Mavrikakis, M. *Surf. Sci.* **2012**, *606*, 1050.

(13) Peng, G.; Sibener, S. J.; Schatz, G. C.; Ceyer, S. T.; Mavrikakis, M. *J. Phys. Chem. C* **2012**, *116*, 3001.

(14) Cavka, J. H.; Jakobsen, S.; Olsbye, U.; Guillou, N.; Lamberti, C.; Bordiga, S.; Lillerud, K. P. *J. Am. Chem. Soc.* **2008**, *130*, 13850.

(15) Garibay, S. J.; Cohen, S. M. *Chem. Commun.* **2010**, *46*, 7700.

(16) Huang, Y.; Qin, W.; Li, Z.; Li, Y. *Dalton Trans.* **2012**, *41*, 9283.

(17) Kim, M.; Cohen, S. M. *CrystEngComm* **2012**, *14*, 4096.

(18) Wu, H.; Yildirim, T.; Zhou, W. *J. Phys. Chem. Lett.* **2013**, *4*, 925.

(19) Valenzano, L.; Civalleri, B.; Chavan, S.; Bordiga, S.; Nilsen, M. H.; Jakobsen, S.; Lillerud, K. P.; Lamberti, C. *Chem. Mater.* **2011**, *23*, 1700.

(20) Biswas, S.; Zhang, J.; Li, Z. B.; Liu, Y. Y.; Grzywa, M.; Sun, L. X.; Volkmer, D.; Van der Voort, P. *Dalton Trans.* **2013**, *42*, 4730.

(21) Yang, Q.; Wiersum, A. D.; Llewellyn, P. L.; Guillerm, V.; Serre, C.; Maurin, G. *Chem. Commun.* **2011**, *47*, 9603.

(22) Yang, Q. Y.; Guillerm, V.; Ragon, F.; Wiersum, A. D.; Llewellyn, P. L.; Zhong, C. L.; Devic, T.; Serre, C.; Maurin, G. *Chem. Commun.* **2012**, *48*, 9831.

(23) Yang, Q.; Wiersum, A. D.; Jobic, H.; Guillerm, V.; Serre, C.; Llewellyn, P. L.; Maurin, G. *J. Phys. Chem. C* **2011**, *115*, 13768.

(24) Yang, Q. Y.; Wiersum, A. D.; Llewellyn, P. L.; Guillerm, V.; Serred, C.; Maurin, G. *Chem. Commun.* **2011**, *47*, 9603.

(25) Pullen, S.; Fei, H.; Orthaber, A.; Cohen, S. M.; Ott, S. *J. Am. Chem. Soc.* **2013**, *135*, 16997.

(26) Luan, Y.; Zheng, N. N.; Qi, Y.; Yu, J.; Wang, G. *Eur. J. Inorg. Chem.* **2014**, 4268.

(27) Cmarik, G. E.; Kim, M.; Cohen, S. M.; Walton, K. S. *Langmuir* **2012**, *28*, 15606.

(28) Vermoortele, F.; Bueken, B.; Le Bars, G.; Van de Voorde, B.; Vandichel, M.; Houthoofd, K.; Vimont, A.; Daturi, M.; Waroquier, M.; Van Speybroeck, V.; Kirschhock, C.; De Vos, D. E. *J. Am. Chem. Soc.* **2013**, *135*, 11465.

(29) Ye, J.; Johnson, J. K. *ACS Catal.* **2015**, *5*, 2921.

(30) Ye, J.; Johnson, J. K.; Li, L. *J. Phys. Chem. C* **2017**, *To be submitted*.